LM-01K032
April 20, 2001

Effect of Substrate Orientation on Phase Separation in Epitaxial GaInAsSb

C.A. Wang, D.R. Calawa, C.J. Vineis

NOTICE

This report was prepared as an account of work sponsored by the United States Government. Neither the United States, nor the United States Department of Energy, nor any of their employees, nor any of their contractors, subcontractors, or their employees, makes any warranty, express or implied, or assumes any legal liability or responsibility for the accuracy, completeness or usefulness of any information, apparatus, product or process disclosed, or represents that its use would not infringe privately owned rights.

Effect of Substrate Orientation on Phase Separation in Epitaxial GaInAsSb

C.A. Wang*, D.R. Calawa, and C.J. Vineis

Lincoln Laboratory, Massachusetts Institute of Technology, Lexington, MA 02420-9108

Abstract

The effect of substrate misorientation on phase separation in $Ga_{1-x}In_xAs_ySb_{1-y}$ nominally lattice-matched to GaSb is reported. The layers were grown at 575 °C by organometallic vapor phase epitaxy on vicinal (001) GaSb substrates, miscut 2° → (-1-11)A, (1-11)B, or (101). $Ga_{1-x}In_xAs_ySb_{1-y}$ ($x \sim 0.1$, $y \sim 0.09$) layers, which have 300-K photoluminescence (PL) peak emission at ~2.1 μm, grow step-bunched and exhibit minimal phase separation. The full width at half maximum of 4-K PL spectra is slightly smaller at 7 meV for layers grown on substrates miscut toward (1-11)B compared to 9 meV for layers grown on substrates miscut toward (-1-11)A and (101). $Ga_{1-x}In_xAs_ySb_{1-y}$ layers with higher alloy composition ($0.16 \leq x \leq 0.19$, $0.14 \leq y \leq 0.17$), which have 300-K PL peak emission at ~2.4 μm, have significant phase separation. These layers are characterized by increased lattice constant variations and epitaxial tilt, broad PL spectra with significant band tailing, and strong contrast modulation in transmission electron microscopy. The degree of decomposition depends on substrate miscut direction: $Ga_{1-x}In_xAs_ySb_{1-y}$ layers grown on (001) 2° → (1-11)B substrates are more homogeneous than those grown on (001) 2° → (-1-11)A and (001) 2° → (101) substrates. The results are attributed to the smaller adatom diffusion length on substrates miscut toward (1-11)B.

Key words: GaInAsSb, phase separation, substrate misorientation, OMVPE

**This work was sponsored by the Department of Energy under AF Contract No. F19628-00-C-0002. The opinions, interpretations, conclusions and recommendations are those of the author and are not necessarily endorsed by the United States Air Force.

1. Introduction

$Ga_{1-x}In_xAs_ySb_{1-y}$ alloys can be grown lattice matched to GaSb or InAs substrates and are useful for a wide range of optoelectronic devices operating in the mid-infrared wavelength region [1-3]. The existence of a large miscibility gap, however, limits the material quality of alloys with x- and y- values that are in the range between approximately 0.15 and 0.85 [4,5]. Since epitaxial layers are typically grown at temperatures between 500 and 600 °C, phase separation by spinodal decomposition is likely. Microscopic compositional inhomogeneities of GaAs- and InSb-rich regions were observed in $Ga_{1-x}In_xAs_ySb_{1-y}$ grown by organometallic vapor phase epitaxy (OMVPE) [6,7]. As a result, the optical, structural, and electrical properties degraded [7,8].

It has been reported that GaInAsSb layers grown by OMVPE are particularly sensitive to growth temperature [4,8-10]. Both optical and structural properties improved by lowering the growth temperature. Furthermore, increasing the growth rate improved optical quality [10]. These results suggest that phase separation can be kinetically limited by reducing adatom diffusion lengths, thus, limiting the ability of the system to achieve equilibrium.

Recently, a study of the surface step structure showed that the decomposition evolves on the surface during epitaxial growth [7,10-11]. GaInAsSb grown on (001) vicinal substrates with a 6° miscut angle had better optical, structural, and electrical properties than layers grown on substrates with a 2° miscut angle [10,11]. However, the miscut directions were not the same. Since both surface diffusion and adatom attachment at step edges are anisotropic on the surface of (001) III-V substrates, [12,13], the

mechanism for the differences in direction is ambiguous. In this paper, the effect of the substrate miscut direction on $Ga_{1-x}In_xAs_ySb_{1-y}$ grown nominally lattice-matched to GaSb substrates by OMVPE is reported.

2. Epitaxial growth and characterization

$Ga_{1-x}In_xAs_ySb_{1-y}$ epitaxial layers were grown nominally lattice matched to vicinal (001) Te-doped GaSb substrates with miscut angles of 2 or 6° → (-1-11)A, (1-11)B, or (101). Step edges of substrates miscut toward (-1-11)A are terminated with group III atoms, A-steps, while substrates miscut toward (1-11)B are terminated with group V atoms, B-steps. Substrates miscut toward (101) have an equal density of A- and B-steps. The GaSb substrates were etched in concentrated HCl for 5 min [14].

Solution trimethylindium, triethylgallium, tertiarybutylarsine, and trimethyl-antimony were used as precursors as described previously [15]. Layers with alloy compositions $0.1 \leq x \leq 0.19$ and $0.09 \leq y \leq 0.17$ grown, with the larger x- and y-values representing alloys deeper in the miscibility gap [4,5]. The growth temperature was 575 °C. Although previous results reported a smaller extent of phase separation for growth at a low temperature of 525 °C, this higher temperature was used to promote a step-bunched surface, which was reported to enhance phase separation [10]. The layers were typically 1 to 2 μm in thickness and grown at ~5 μm/h. A vertical rotating-disk OMVPE reactor was used with H_2 carrier gas at a flow rate of 10 slpm, reactor pressure of 150 Torr, and typical rotation rate of 40 rpm.

The layers were characterized with atomic force microscopy (AFM) operated in tapping mode. Etched Si cantilevers with a nominal tip radius of 5 to 10 nm and a

sidewall angle of 10° were used. The structural quality was evaluated by transmission electron microscopy (TEM) and high-resolution x-ray diffraction (HRXRD), while PL measurements at 4 and 300 K were used to characterize the optical properties.

3. Results

Figure 1 shows AFM images of $Ga_{1-x}In_xAs_ySb_{1-y}$ layers with two nominally different alloy compositions grown on (001) 2° → (-1-11)A, (001) 2° → (1-11)B, and (001) 2° → (101) substrates. The alloy composition was estimated from XRD and 300-K photoluminescence (PL). AFM images of layers with x ~ 0.1 and y ~ 0.09, which corresponds to ~2.1-μm GaInAsSb, are shown in Figs. 1a, 1b, and 1c. All surfaces exhibit a periodic morphology that is attributed to step-bunching [16,17]. The step edges are aligned perpendicular to the miscut direction. The average width of (001) terraces vary from about 39, 35, and 43 nm for the (001) 2° → (-1-11)A, (001) 2° → (1-11)B, and (001) 2° → (101) substrates, respectively, and step heights vary accordingly to preserve the substrate miscut angle of about 2°. Larger scale height undulations with a periodicity of about 150 nm are observed for layers grown on the (001) 2° → (1-11)B and (001) 2° → (101) substrates. These undulations are not always present [10], and are related to vertical composition modulations that are tilted with respect to the miscut surface [18].

AFM images of layers with higher alloy compositions, x ≥ 0.16, y ≥ 0.14, are shown in Figs. 1d, 1e, and 1f. The 300-K PL emission corresponds to 2.4 μm for the samples in Figs. 1d, and 1e, and 2.3 μm for that in Fig. 1f. The layers are at various stages in breakdown of the surface structure, and the periodic step-bunches has broken up into an irregular morphology. The miscut direction of the original substrate is only evident

for the layers grown on (001) 2° → (-1-11)A and (001) 2° → (1-11)B substrates. GaInAsSb grown on (001) 2° → (101) exhibits relatively large (100 to 500 nm) flat regions separated by narrow trenches that are several nanometers deep and aligned nearly parallel with [-110]. Previously, it was reported that compared to the average composition these narrow trenches corresponded to regions that were as much as 2 to 3 atomic percent GaAs-rich, while the larger regions were InSb-rich [6,7].

TEM studies of GaInAsSb cross-sectional samples using <220> diffraction conditions show contrast modulation [18] that is indicative of spinodal-like decomposition [13,19]. $Ga_{0.9}In_{0.1}As_{0.09}Sb_{0.91}$ layers have very faint contrast modulation which is indistinguishable in layers grown on substrates with the three different miscut directions. Strong contrast modulation is observed in $Ga_{1-x}In_xAs_ySb_{1-y}$ with $x \geq 0.16$, $y \geq 0.14$, and it is distinctly different depending on the miscut direction. Layers grown on (001) 2° → (1-11)B substrates show less contrast than those grown on (001) 2° → (-1-11)A, while those grown on (001) 2° → (101) have the most contrast.

Figure 2 shows HRXRD reciprocal space maps of $Ga_{0.9}In_{0.1}As_{0.09}Sb_{0.91}$ grown on (001) 2°→(1-11)B and $Ga_{1-x}In_xAs_ySb_{1-y}$ with $x \geq 0.16$, $y \geq 0.14$ on substrates with the three different miscut directions. HRXRD of $Ga_{0.9}In_{0.1}As_{0.09}Sb_{0.91}$ grown on (001) 2°→(-1-11)A and (001) 2°→(101) substrates are similar to that on (001) 2°→(1-11)B. It is evident that all layers are nominally lattice-matched to the GaSb substrate. There are, however, varying degrees of strain due to lattice constant variations and epitaxial tilt associated with these layers. Both strain and tilt are negligible for $Ga_{0.9}In_{0.1}As_{0.09}Sb_{0.91}$ layers. On the other hand, $Ga_{1-x}In_xAs_ySb_{1-y}$ layers with $x \geq 0.16$, $y \geq 0.14$ are extremely

inhomogeneous. Compressive and tensile strain, which is probably associated with GaAs-rich and InSb-rich quaternaries, is nearly symmetric and apparently is balanced. GaInAsSb grown on (001) 2° → (1-11)B exhibits the smallest tilt and narrowest range of lattice constant, while these parameters increase for (001) 2° → (-1-11)A and further still for (001) 2° → (101).

The 4- and 300-K PL spectra of $Ga_{0.9}In_{0.1}As_{0.09}Sb_{0.91}$ grown on (001) 2°→(1-11)B is shown in Fig. 3a. The PL spectra of $Ga_{0.9}In_{0.1}As_{0.09}Sb_{0.91}$ grown on (001) 2°→(-1-11)A and (001) 2°→(101) substrates are similar, and Table 1 summarizes the PL data for those samples shown in Fig. 1a – 1c. The 4-K PL FWHM value provides a semi-quantitative measure of the degree of phase separation [10,13]. The FWHM values are 9.0, 7.2, and 9.3 meV for (001) 2° → (-1-11)A, (1-11)B, and (101) substrates, respectively. Thus, these results indicate that the most homogeneous alloy is obtained for the layer grown on (001) 2° → (1-11)B, while similar quality is obtained for layers grown on (001) 2° → (-1-11)A and (001) 2° → (101). All samples show that the difference between the 4- and 300-K PL peak energy ($E_{4\text{-}300K}$) is ~74 meV, which corresponds to the expected difference based on the energy gap dependence on temperature.

Table 1 also lists PL data of $Ga_{0.9}In_{0.1}As_{0.09}Sb_{0.91}$ grown on substrates with a 6° miscut angle in the three different miscut directions. In all cases, the 4-K PL FWHM values are smaller for layers grown with the larger miscut angle. AFM measurements indicated smaller terrace widths (~22 nm) for layers grown on the 6° miscut substrates.

The 4- and 300-K PL spectra of $Ga_{1-x}In_xAs_ySb_{1-y}$ layers with $x \geq 0.16$, $y \geq 0.14$ are shown in Figs. 3b-d and the data are summarized in Table 1.The 4-K PL FWHM values

are considerably larger at 36.1, 13.6 and 42.0 meV for layers on (001) 2° → (-1-11)A, (001) 2° → (1-11)B, and (001) 2° → (101) substrates, respectively. Band tailing is especially significant for layers grown on (001) 2° → (-1-11)A and (001) 2° → (101) substrates. The PL properties of $Ga_{0.81}In_{0.19}As_{0.17}Sb_{0.83}$ grown on (001) 2° → (1-11)B, which also has the highest x- and y-values, are significantly better. $E_{4\text{-}300K}$ is 68 meV for this substrate miscut, compared to only about 18 meV for (001) 2° → (-1-11)A and (001) 2° → (101). The red-shift of 4-K PL spectra is due to recombination in the smaller band-gap InSb-rich regions [10,13].

4. Discussion

The results show that the miscut direction of (001) GaSb substrates is an important parameter in determining the extent of phase separation, and thus epilayer quality, of GaInAsSb grown by OMVPE. Alloy decomposition results in microscopic compositional variations that ultimately increase in magnitude to severely disrupt the smooth step-flow growth of step-bunched surfaces. Correspondingly, structural and optical properties reflect this alloy inhomogeneity, and are characterized by irregular step structure, increasing contrast modulation in TEM, and increasing linewidths of XRD and PL. Properties degrade as the extent of phase separation increases. Furthermore, phase separation is more limited in GaInAsSb layers grown on (001) 2° → (1-11)B substrates, which are consistently more homogeneous compared to layers of similar composition grown on (001) 2° → (-1-11)A or (001) 2° → (101) substrates.

Phase separation proceeds on the surface during epitaxial growth, and as such is sensitive to kinetic factors including temperature, adatom flux, and substrate surface

orientation [7,10-11,20-21]. When the rate of adatom incorporation at step edges increases, adatom clustering on (001) terraces is reduced, and thus phase separation is limited. The AFM results indicate that adatom diffusion lengths are dependent on substrate miscut angle and direction. Substrates with a large miscut angle have a small terrace width. Layers grown on (001) substrates miscut toward (1-11)B have the smallest terrace widths and (001) substrates miscut toward (101) have the largest terrace widths. Consequently, GaInAsSb grown on substrates with a 6° miscut angle have better PL properties than those on substrates with a 2° miscut angle. In addition, layers grown on (001) substrates miscut toward (1-11)B have the least phase separation, while (001) substrates miscut toward (101) have the most phase separation.

The step structure, since it is affected by growth kinetics, appears to be a dominating factor in determining phase separation. Although the atomic bonding and reconstructions are unknown for GaSb-based materials grown by OMVPE, especially at step edges, the results indicate that there is preferential incorporation of adatoms at B-step edges. This result is consistent with previous reports that the Ga sticking coefficient was higher for GaSb grown on substrates miscut toward the B surface compared to those toward the A surface [22].

Since (001) substrates miscut toward (101) have both A- and B-step edges, another mechanism that has to be considered is the surface diffusion rate. The AFM image shown in Fig. 1f indicates a surface structure with trenches aligned in the [-110] direction. These trenches are associated with GaAs-rich regions, and stronger composition modulation is observed along the [110]. Therefore, the adatom diffusion

length is larger in the [110] direction compared to [-110] on the (001) surface [23]. The limiting factor then, is diffusion along [110]. The diffusion length on (001) 2° → (101) substrates is increased by at least the square root of 2, in addition to the nominally longer terrace width observed on these substrates. The extent of phase separation is largest on these substrates.

5. Conclusions

In conclusion, the substrate misorientation has a significant effect on phase separation in GaInAsSb grown by OMVPE. It was found that growth on (001) 2° → (1-11)B substrates limits phase separation compared to that on (001) 2° → (-1-11)A or (001) 2° → (101) substrates. Thus, the onset of the surface deterioration and degradation of optical and structural properties can be limited by growing on substrates miscut toward (1-11)B. Increasing the miscut angle also reduces phase separation. The results are explained by the smaller adatom diffusion length on these substrates.

Acknowledgments

The authors gratefully acknowledge J.W. Chludzinski for photoluminescence measurements and D.C. Oakley for technical assistance in epitaxial growth. This work was sponsored by the Department of Energy under AF Contract No. F19628-00-C-0002. The opinions, interpretations, conclusions, and recommendations are those of the author and are not necessarily endorsed by the U.S. Air Force.

References

1. Y. Tian, B. Zhang, T. Zhou, H. Jiang, Y. Jin, Phys. Stat. Sol. A 174 (1999) 413.
2. D. Garbuzov, M. Maiorov, H. Lee, V. Khalfin, R. Martinelli, J.Connolly, Appl. Phys. Lett. 74 (1999) 2990.
3. G.W. Charache, P.F. Baldasaro, L.R. Danielson, D.M. Depoy, M.J. Freeman, C.A. Wang, H.K. Choi, D.Z. Garbuzov, R.U. Martinelli, V. Khalfin, S. Saroop, J.M. Borrego, R.J. Gutman, J. Appl. Phys. 85 (1999) 2247.
4. M.J. Cherng, H.R. Jen, C.A. Larsen, G.B. Stringfellow, H. Lundt, P.C. Taylor, J. Cryst. Growth 77 (1986) 408.
5. K. Onabe, Jap. J. Appl. Phys. 21 (1982) L323.
6. C.A. Wang, H.K. Choi, S.L. Ransom, G.W. Charache, L.R. Danielson, D.M. DePoy, Appl. Phys. Lett. 75 (1999) 1305.
7. C.A. Wang, D.R. Calawa, C.J. Vineis, J. Cryst. Growth 2001 Evolution of Surface Structure and Phase Separation in GaInAsSb
8. C.A. Wang, H.K. Choi, G.W. Charache, IEE Proc.-Optoelectron. 147 (2000) 193.
9. M. Sopanen, T. Koljonen, H. Lipsanen, T. Tuomi, J. Cryst. Growth 145 (1994) 492.
10. C.A. Wang, Appl. Phys. Lett. 76 (2000) 2077.
11. C.A. Wang, J. Electron. Mater. 29 (2000) 112.
12. H. Asai, J. Cryst. Growth 80 (1987) 425.
13. R.R. LaPierre, T. Okada, B.J. Robinson, D.A. Thompson, G.C. Weatherly, J. Cryst. Growth 155 (1995) 1.

14. C.J. Vineis, C.A. Wang, K.F. Jensen, J. Cryst. Growth 2001 In-Situ Reflectance Monitoring of GaSb Substrate Oxide Desorption
15. C.A. Wang, J. Cryst. Growth 191 (1998) 631.
16. M. Kasu, N. Kobayashi, Appl. Phys. Lett. 62 (1993) 1262.
17. M. Shinohara, N. Inoue, Appl. Phys. Lett. 66 (1995) 1936.
18. C.J. Vineis PhD Thesis
19. A. Zunger, S. Mahajan, in Handbook on Semiconductors Vol. 3, ed. S. Mahajan, North Holland, New York, 1994, p. 1399.
20. T.L. McDevitt, S. Mahajan, D.E. Laughlin, W.A. Bonner, V.G. Keramidas, Phys. Rev. B 45 (1992) 6614.
21. R.R. LaPierre, B.J. Robinson, D.A. Thompson, Appl. Surf. Sci. 90 (1995) 437.
22. N. Bertru, M. Nouaoura, J. Bonnet, L. Lassabatere, J. Cryst. Growth 160 (1996) 1.
23. J.-S. Liu, J.-S. Wang, K.Y. Hsieh, and H.-H. Lin, J. Cryst. Growth 206 (1999)15.

Figure Captions

Figure 1. Atomic force microscope images of (a) $Ga_{0.9}In_{0.1}As_{0.09}Sb_{0.91}$ on (001) 2° →(-1-11)A, (b) $Ga_{0.9}In_{0.1}As_{0.09}Sb_{0.91}$ on (001) 2° →(1-11)B, (c) $Ga_{0.9}In_{0.1}As_{0.09}Sb_{0.91}$ on (001) 2° →(101), (d) $Ga_{0.82}In_{0.18}As_{0.16}Sb_{0.84}$ on (001) 2° →(-1-11)A, (e) $Ga_{0.81}In_{0.19}As_{0.17}Sb_{0.83}$ on (001) 2° →(1-11)B, and (f) $Ga_{0.84}In_{0.16}As_{0.14}Sb_{0.86}$ on (001) 2° →(101). Vertical scale is 5 nm/division in all cases.

Figure 2. High resolution x-ray diffraction of (a) $Ga_{0.9}In_{0.1}As_{0.09}Sb_{0.91}$ on (001) 2° →(1-11)B, (b) $Ga_{0.82}In_{0.18}As_{0.16}Sb_{0.84}$ on (001) 2° →(-1-11)A, (c) $Ga_{0.81}In_{0.19}As_{0.17}Sb_{0.83}$ on (001) 2° →(1-11)B, and (d) $Ga_{0.84}In_{0.16}As_{0.14}Sb_{0.86}$ on (001) 2° →(101).

Figure 3. Photoluminescence spectra measured at 4 and 300 K of (a) $Ga_{0.9}In_{0.1}As_{0.09}Sb_{0.91}$ on (001) 2° →(1-11)B, (b) $Ga_{0.82}In_{0.18}As_{0.16}Sb_{0.84}$ on (001) 2° →(-1-11)A, (c) $Ga_{0.81}In_{0.19}As_{0.17}Sb_{0.83}$ on (001) 2° →(1-11)B, and (d) $Ga_{0.84}In_{0.16}As_{0.14}Sb_{0.86}$ on (001) 2° →(101).

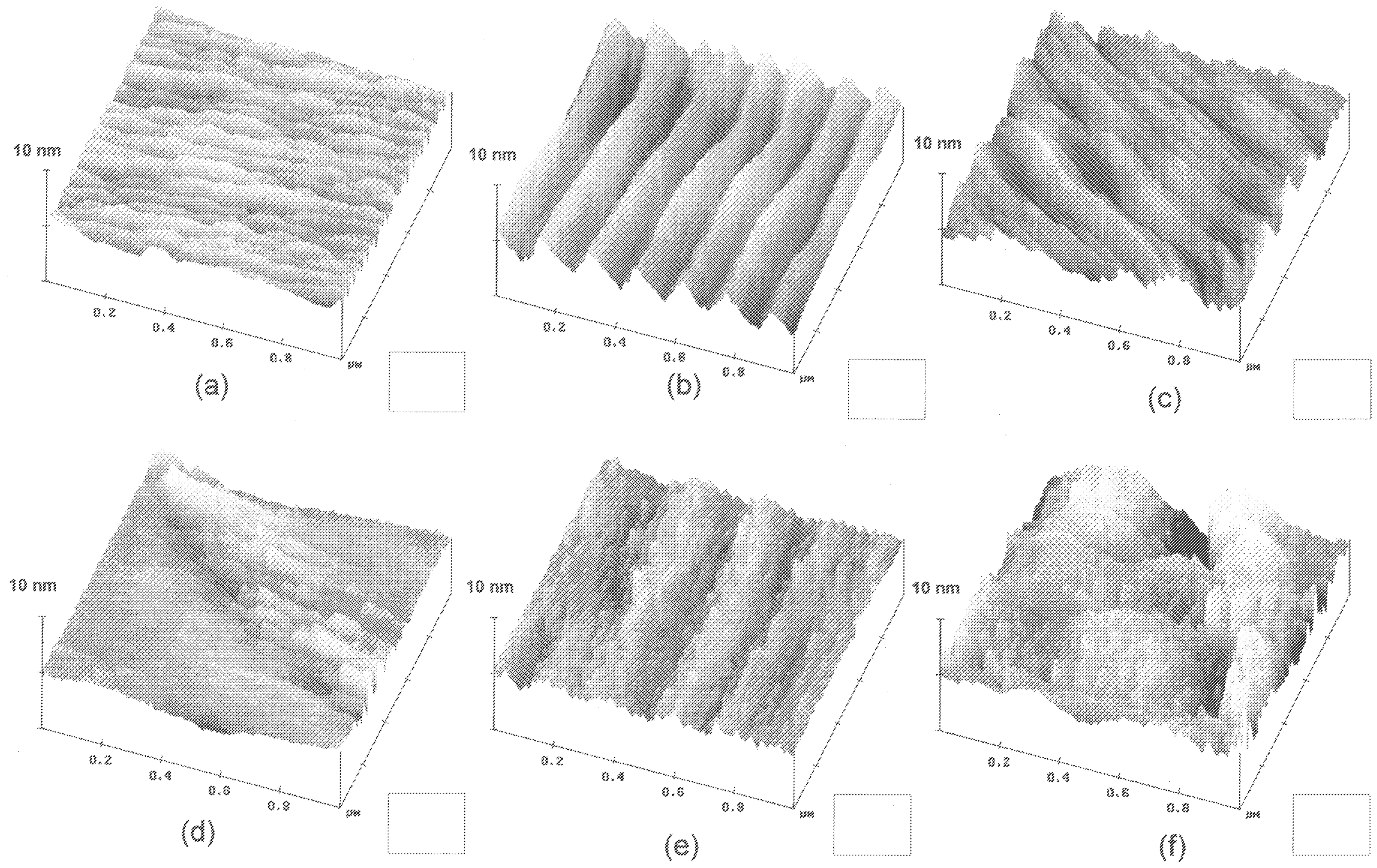

Figure 1

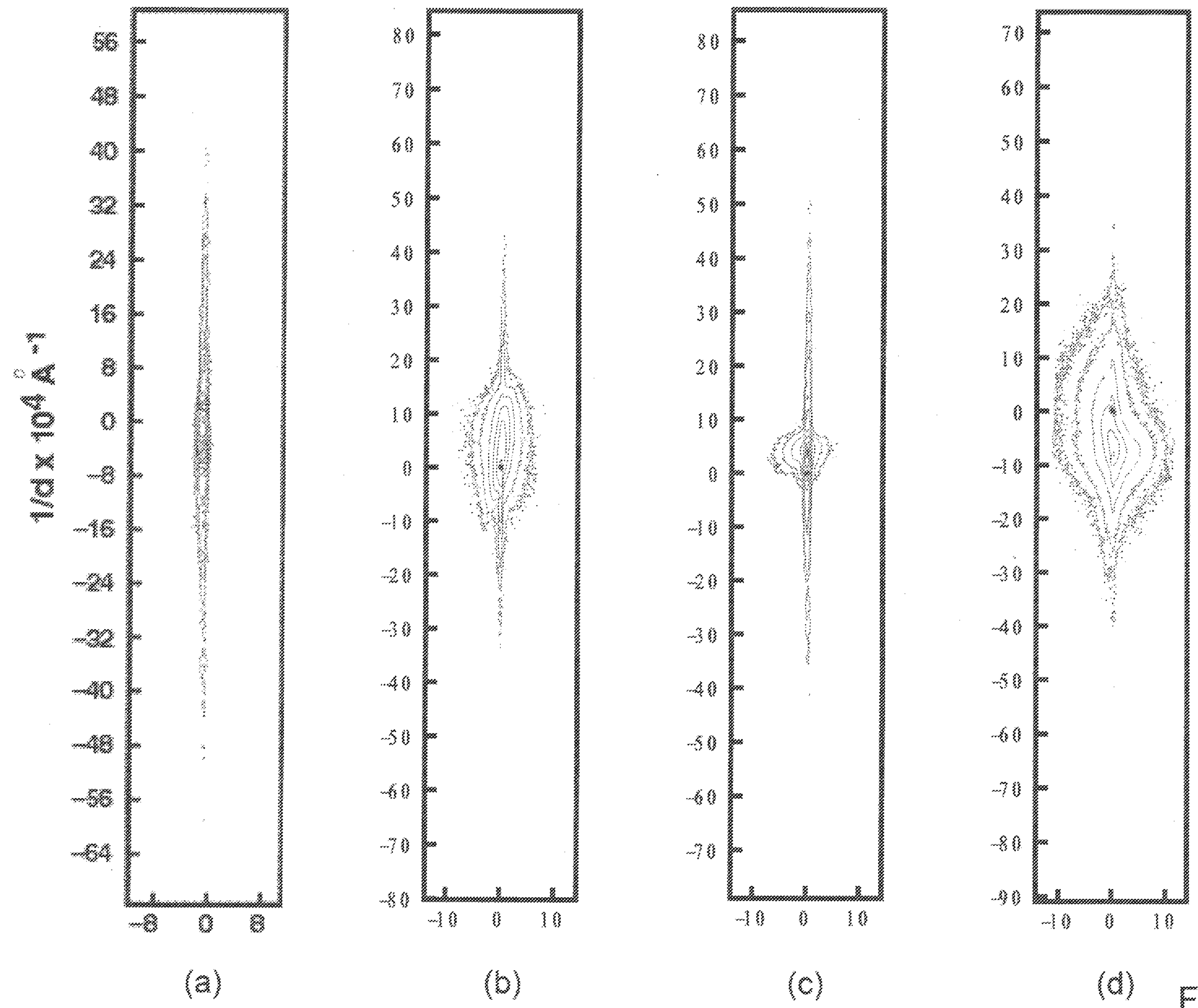

Figure 2

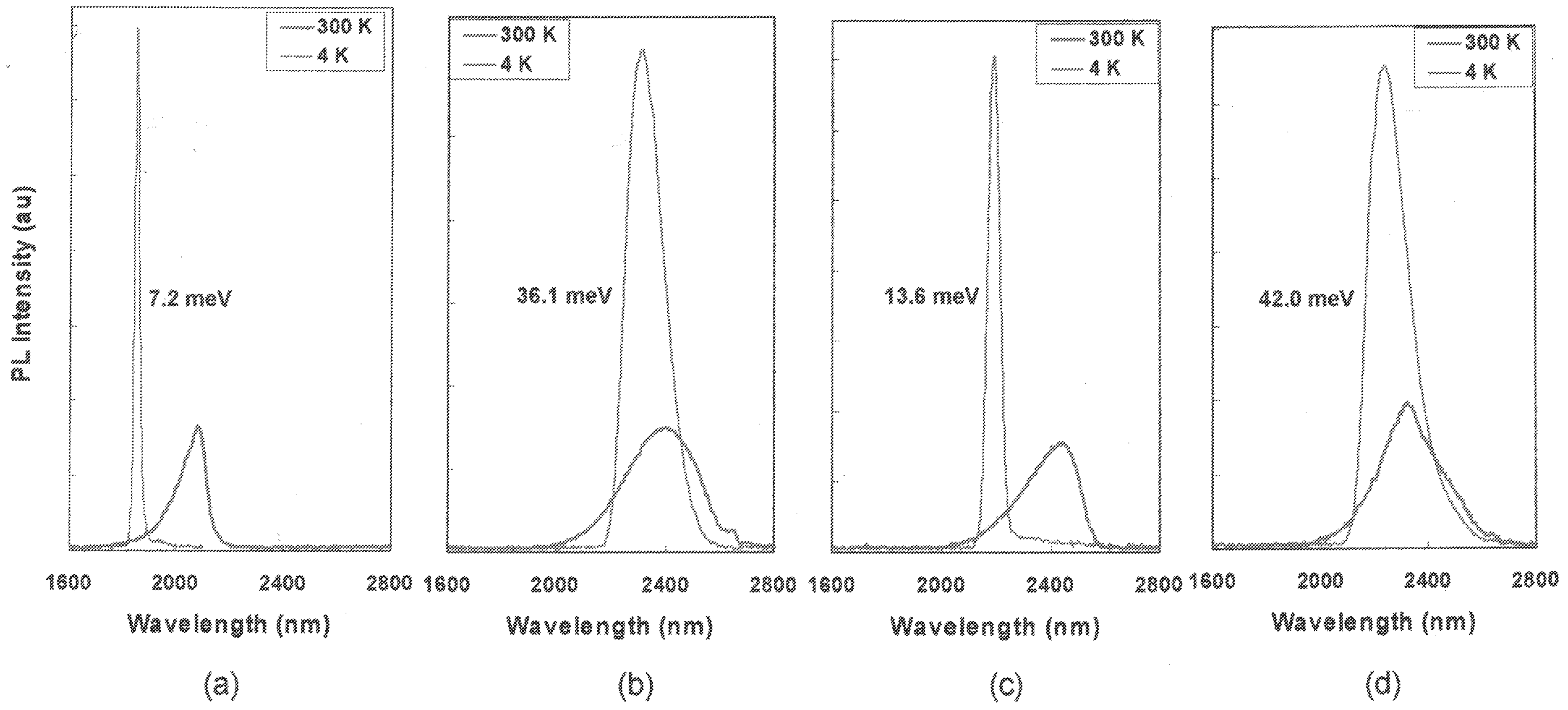

Figure 3

15

Table 1. Photoluminescence data of GaInAsSb

Substrate	300 K PL (nm)	4 K PL (nm)	$E_{4\text{-}300K}$ (meV)	4 K PL FWHM (meV)
(001) $2^{\circ} \rightarrow$ (-1-11)A	2088	1856	74.2	9.0
(001) $2^{\circ} \rightarrow$ (1-11)B	2080	1849	74.5	7.2
(001) $2^{\circ} \rightarrow$ (101)	2088	1858	73.5	9.3
(001) $2^{\circ} \rightarrow$ (-1-11)A	2397	2313	1.9	36.1
(001) $2^{\circ} \rightarrow$ (1-11)B	2441	2192	57.7	13.6
(001) $2^{\circ} \rightarrow$ (101)	2315	2238	1.8	42.0
(001) $6^{\circ} \rightarrow$ (-1-11)A	2090	1860	73.4	5.7
(001) $6^{\circ} \rightarrow$ (1-11)B	2082	1857	72.2	6.1
(001) $6^{\circ} \rightarrow$ (101)	2065	1844	72.0	5.8